

# Texture-based analysis of hydrographical basins with multispectral imagery

Pedro G. Bascoy<sup>a</sup>, Alberto S. Garea<sup>a</sup>, Dora B. Heras<sup>a</sup>, Francisco Argüello<sup>b</sup>, and Álvaro Ordóñez<sup>a</sup>

<sup>a</sup>Centro Singular de Investigación en Tecnologías Inteligentes (CiTIUS), Universidade de Santiago de Compostela, Santiago de Compostela, Spain

<sup>b</sup>Departamento de Electrónica e Computación, Universidade de Santiago de Compostela, Santiago de Compostela, Spain

## ABSTRACT

In this paper the problem of studying the presence of different vegetation species and artificial structures in the riversides by using multispectral remote sensing information is studied. The information provided contributes to control the water resources in a region in northern Spain called Galicia. The problem is solved as a supervised classification computed over five-band multispectral images obtained by an Unmanned Aerial Vehicle (UAV). A classification scheme based on the extraction of spatial, spectral and textural features previous to a hierarchical classification by Support Vector Machine (SVM) is proposed. The scheme extracts the spatial-spectral information by means of a segmentation algorithm based on superpixels and by computing morphological operations over the bands of the image in order to generate an Extended Morphological Profile (EMP). The texture features extracted help in the classification of vegetation classes as the spatial-spectral features for these classes are not discriminant enough. The classification is computed over segments instead of pixels, thus reducing the computational cost. The experimental results over four real multispectral datasets from Galician riversides show that the proposed scheme improves over a standard classification method achieving very high accuracy results.

**Keywords:** vegetation, unmanned aerial vehicles, multispectral, classification, textures, superpixel, support vector machine.

## 1. INTRODUCTION

Monitoring vegetation changes is essential in the context of current climatic change conditions and rapid human interventions. Remotely sensed information of the vegetation species present in a region, and the dynamic behavior of that vegetation provides very useful insights for environmental monitoring, biodiversity conservation, agriculture, forestry, and many other fields. Satellite based remote sensing is, in some cases, a cost effective solution as long time data series of consistent and comparable data are usually provided by the sensors placed on these platforms.<sup>1</sup> Nevertheless, UAVs provide a much more flexible platform with a revisiting time of the same region that can be tuned, and a higher spatial resolution at lower costs.

Vegetation information from remotely sensed images is mainly interpreted by differences and changes in the green color of the leaves. Very simple methods such as the calculation of vegetation indices, e.g. Normalized Difference Vegetation Index (NDVI),<sup>1</sup> are calculated by combining two or three bands obtained by multispectral or hyperspectral sensors. But these indices are not suitable for the separation of vegetation species. Neural networks have become popular in the analysis of remote sensing data showing their efficiency for a variety of problems.<sup>2</sup> For the particular case of vegetation identification from UAV remote sensing images, Senthilnath et al.<sup>3</sup> propose a classification method for tree crown classification based on a spectral-spatial method, in particular, a hierarchical clusterisation method based on k-means and expectation maximization. In the case of Feng et al.,<sup>4</sup> random forest is used for urban vegetation mapping together with texture analysis, showing that using texture features improves the classification accuracy significantly.

---

Further author information: E-mail: [{pedro.gonzalez.bascoy, dora.blanco, francisco.arguelloalvaro.ordonez}@usc.es](mailto:{pedro.gonzalez.bascoy,dora.blanco,francisco.arguelloalvaro.ordonez}@usc.es)

Remote Sensing for Agriculture, Ecosystems, and Hydrology XXI, edited by Christopher M. U. Neale, Antonino Maltese, Proc. of SPIE Vol. 11149, 111490Q · © 2019 SPIE  
CCC code: 0277-786X/19/\$21 · doi: 10.1117/12.2532760

The overall objective of this paper is to detect the presence not only of different vegetation species but also non-vegetation elements along the riverside and a region of around 100 meters on both sides of the river, as a first step in visualizing changing vegetation dynamics over time. With this aim, a supervised classification methods based on spatial-spectral and textural features is proposed.

## 2. SPATIAL-SPECTRAL TEXTURE-BASED CLASSIFICATION SCHEME

The problem of identifying different vegetal species and non-vegetal structures is posed in this paper as a supervised classification problem. In order to address it, a spectral-spatial texture-based classification scheme is proposed. As it is well-known in the remote sensing field, the classification results are improved when information on the spatial structures present in the input image is added to the different spectral features available for each pixel of the image.<sup>5</sup> In the case of identifying different vegetation species, the textural information helps to discriminate among different species with very similar spectral signatures, i.e., similar reflectance values.<sup>6</sup>

Figure 1 shows the classification scheme proposed in this paper. The steps involved in the scheme are the following:

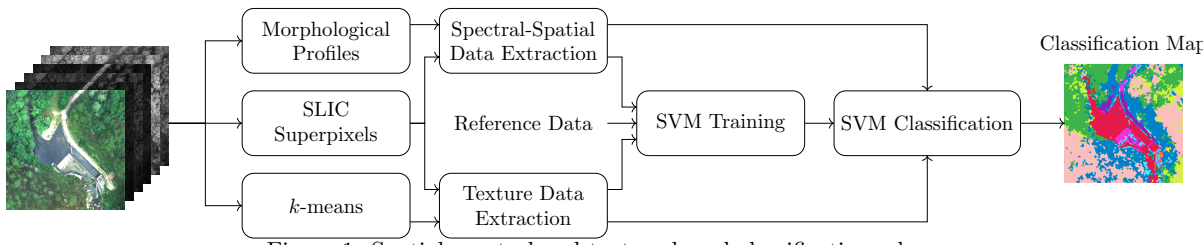


Figure 1: Spatial-spectral and texture-based classification scheme.

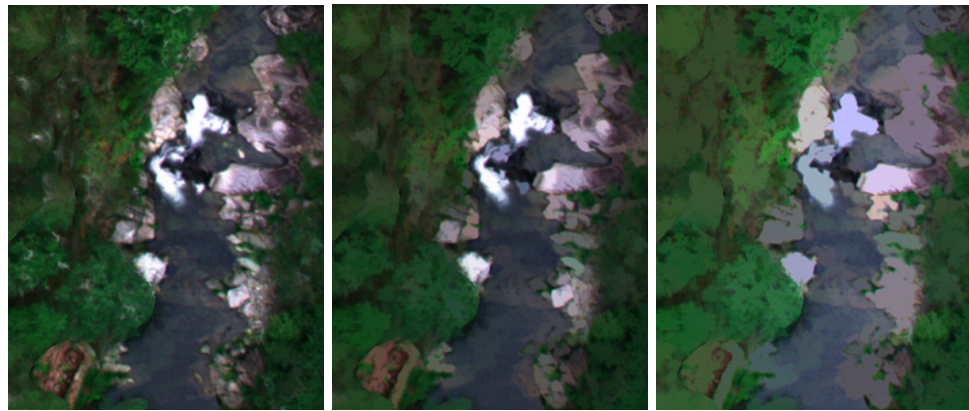
1. **Morphological Profiles:** First, extended morphological profiles (EMPs)<sup>7,8</sup> are generated. As a result, from the bands of the image new bands including spatial information at different sizes are created through mathematical morphology operations. In this particular approach, the transformations performed are morphological openings and closings with a structuring element (SE) of increasing size. As a result, for each band of the image the different dim and bright structures in the band are highlighted. The classifiers take advantage of two side effects of the spatial enhancing produced by the EMPs: the reduction of noise and the homogeneity increase in the neighborhood of each pixel.

Figure 2 shows the effect that the EMP calculation produces over a portion of a river bank image when the radius of the SE is increased. As the radius increases, the influence of the small spatial structures is also decreased. In Figure 2, rocks and tree crowns in the river bank are simplified into larger structures.

2. **SLIC Superpixels:** its objective is the identification and delimitation of uniform regions. Superpixel segmentation algorithms such as SLIC<sup>9</sup> are able to split the image into segments of similar size, adapting its shape to the natural borders of spatial structures in the image. Some advantages of SLIC over other segmentation algorithms include the possibility to tune the parameters that influence the characteristics of the segments (allowing to tune segment sizes, change the regularisation factor and set minimum size constraints), and its low execution time.

In the scheme, SLIC plays two key roles: a data downsizer and a spectral-spatial structure enhancer. Some algorithms in the scheme that are executed after SLIC, such as SVM, are computed over segments instead of over separate pixels. An example of a segmented scene can be seen in Figure 3.

3. **k-means:** a clusterisation algorithm such as *k*-means<sup>10,11</sup> is actually an unsupervised classifier that separates pixels into a number of classes based on the criteria selected by the user. The *k*-means algorithm uses the Euclidean distance between the centroids (as many as the number of clusters) as separation criterion. These are iteratively updated as the average of all the nearest pixels to its current position. In the proposed solution, pixels of the training images are assigned a membership to a cluster of a total decided by the user.



(a) Original color composition. (b) Disk of radius 5 as SE. (c) Disk of radius 10 as SE.

Figure 2: Example of the effect of morphological transformations with different sizes of the SE in a river bank.

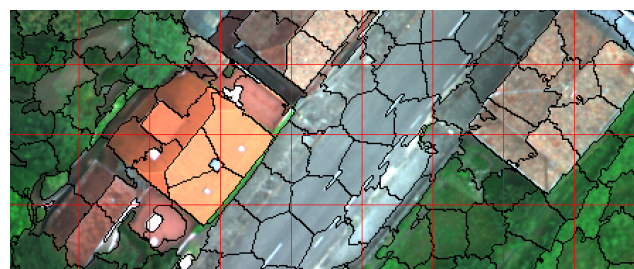
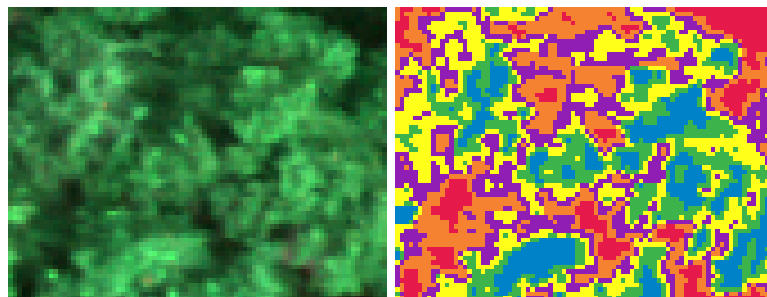


Figure 3: Resulting SLIC segmentation with a selected average segment size of 100 pixels.

In Figure 4 the resulting unsupervised classification of an oak canopy is shown. As can be seen, the membership distribution is helpful to determine the vegetation species, since different types of tree crowns often provide unique membership layouts.



(a) Oak canopy color composite. (b) Example of k-means application.

Different colors represent memberships to different clusters.

Figure 4: *k*-means clusterisation of an oak crown into 6 clusters.

- 4. Spectral-Spatial Data Extraction:** the goal of this stage is to combine the EMP and the superpixel segmentation map. For each segment and each band of the image calculated from the EMP, the average and standard deviation values for the pixels in the segment are calculated. This approach of fusing spectral and spatial information makes the scheme highly reliable against misregistered and noisy regions while reducing the computational requirements by one to two orders of magnitude, depending on the segment average size.

**5. Texture Data Extraction:** the purpose of this stage is to extract the variation of individual pixels inside segments, i.e. texture features, to distinguish among vegetation canopies. In the proposed scheme  $k$ -means plays the role of a simplified version of the Fisher Vector (FV)<sup>13</sup> approach achieving similar performance and allowing the characterisation of superpixels by membership statistics that are not sensible to scale and rotation.

Figure 5 shows an example of application to an image (Figure 5a) made up of oak (on the left) and eucalyptus (on the right) canopies. The clusterisation map of Figure 5b shows that, as expected, the membership distribution among the eucalyptus and oak crowns is remarkable different.

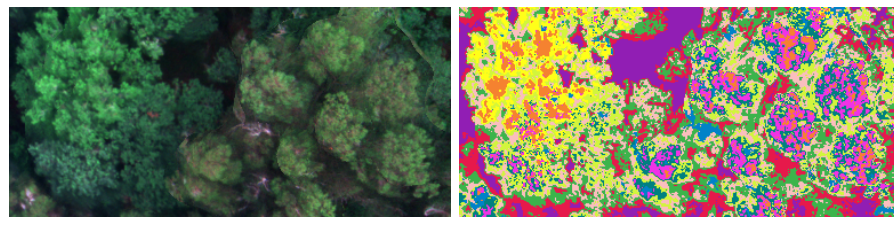


Figure 5: A color composition scene of oak and eucalyptus canopies and its clusterisation with  $k$ -means using 10 classes.

**6. SVM Classification:** the spectral-spatial and texture features extracted in the previous stages feed four SVM classifiers that are hierarchically arranged. The objective of this hierarchy, shown in Figure 6, is to discriminate first into large groups that are easier to classify because their spectral signatures are very different. Figure 6a shows the different classification models created by the different SVMs after the training step. The operation of the classification hierarchy is shown in 6b. The inputs to SVM 1, SVM 2, and SVM 3 that perform the identification of vegetation, water and non-vegetation classes, respectively, are the spectral-spatial features. Due to the fact that the separation among vegetation species is a more challenging task, the inputs to SVM 4 are the texture features.

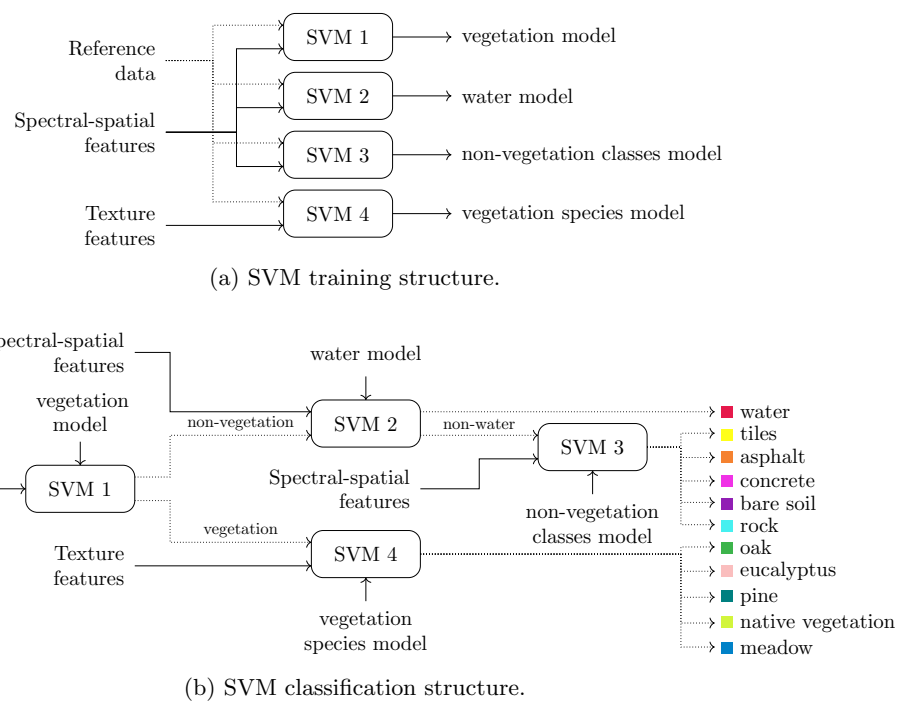


Figure 6: SVM training and classification hierarchies.

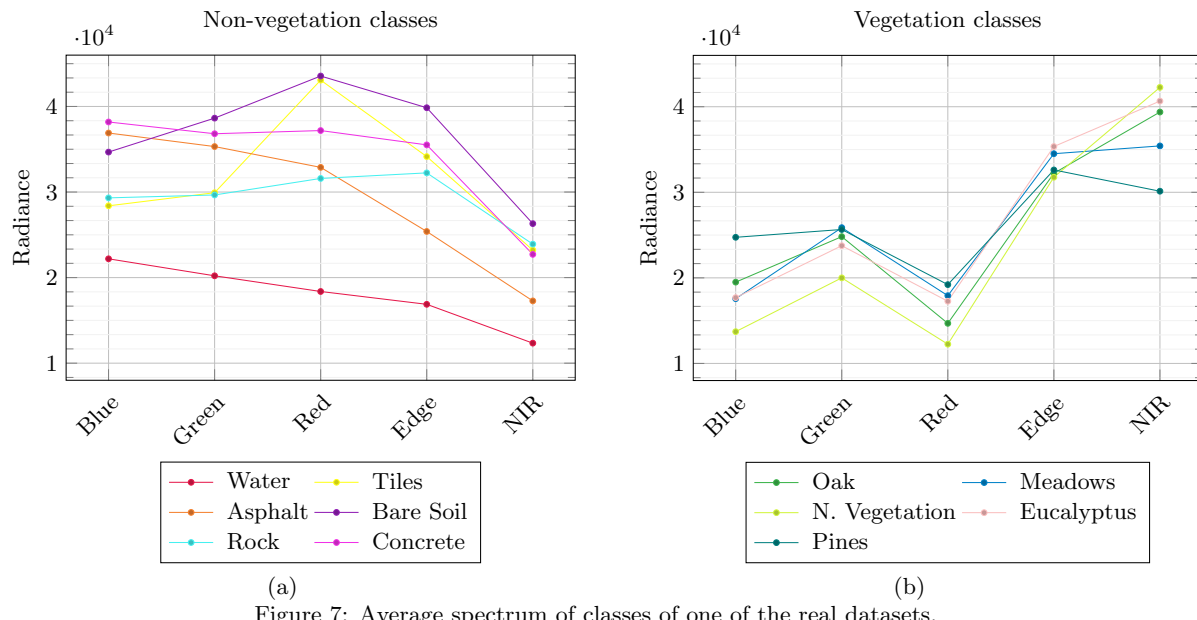


Figure 7: Average spectrum of classes of one of the real datasets.

Figure 7 shows the variability of the spectral signatures for the different classes for the Eiras Dam dataset. In particular, Figures 7a and 7b show the average spectrum of non-vegetation and vegetation classes respectively, evidencing that a separation between non-vegetation and vegetation classes is a straightforward task as compared to the separation of the eleven classes altogether.

### 3. DATASET DESCRIPTION

In this section the four multispectral datasets used in the experiments are described as well as other relevant technical information.

#### 3.1 Locations and sensor

With the objective of monitoring the interaction of the masses of native vegetation (N. Vegetation) with artificial structures and river beds, four locations in the Galician province of Pontevedra were selected. These are located in an area comprised between the “Embalse do Eiras” (Eiras dam) location and the local village of “Pizargos”, with a distance of approximately 13 kilometers end-to-end. They were selected based on the presence of native vegetation, Eucalyptus (*Eucalyptus globulus*), and maritime pine (*Pinus pinaster*). The native vegetation, that populates areas near the water streams due to its ability to survive under unstable water conditions, includes oaks (*Quercus robur* and *Quercus pyrenaica*), birches (*Betula pendula*), alders (*Alnus glutinosa*), and willows. Different artificial structures are also present and are identified: rooftops covered by tiles, some concrete structures, asphalt roads, stone structures, and bare soil roads.

The datasets were captured by the MicaSense RedEdge multispectral camera mounted on a custom UAV. Its five discrete sensors provide spectral channels at wavelengths of 475 nm (Blue), 560 nm (Green), 668 nm (Red), 717 nm (Edge), and 840 nm (NIR). The spatial resolution is 8.2 cm/pixel at a height of 120 m. The sensor is placed on a UAV, allowing the capture of data over long distances in each flight.

#### 3.2 Datasets

Four datasets were captured in four different zones in the basins of the rivers Oitavén and Xesta:

- River Oitavén: this dataset captures the watershed of the river Oitavén on its way through the local village A Ponte. It was photographed on July 18, 2018 at a height of 120 meters. The size of the image is  $6689 \times 6722$  pixels and its color composite can be seen in Figure 8a. It reveals some misregistered areas in the lower right part of the scene, probably caused by the unpredictable light variations along the flight. Leaving aside those artifacts, the image is indeed in very good shape. In it, several tree species (oak and eucalyptus are specially abundant) and a number of artificial structures can be spotted.
- Creek Ermidas: 500 meters east from the River Oitavén dataset, the Creek Ermidas meets the river Oitavén. The flight, carried out on July 18, 2018 at a height of 120 m, covers the banks where these two water flows converge, as depicted in Figure 8c. The dimensions of this dataset are  $11924 \times 18972$  pixels and present some shaded areas in the surroundings of the main road crossing the image from north to south. In relation to the vegetation masses, there are plenty of oak and eucalyptus canopies on the west whereas the east side is sparsely populated by pines.
- Xesta Basin: near the border between the Galician provinces of Pontevedra and Ourense is located the source of the River Xesta. This is an exquisitely preserved basin with vast fields of low vegetation, unique rocky areas as well as oak canopies. The images were captured on July 6, 2018 at a height of 120 m. The RGB composition of the mosaic is shown in Figure 8e and it has a resolution of  $15424 \times 10179$  pixels.
- Eiras Dam: finished in 1977, Eiras dam is the reservoir that supplies running water to the town of Vigo. The dam outlet gives way to a river bed with many meanders, surrounded to the south by dense oak canopies and artificial paths. The lack of vegetation that can be noticed on the north banks was due to a fire that took place in 2018. To the east, the dam crest along the main penstock appear bounded by some sparse pines crowns. The image dimensions are  $5176 \times 18224$  pixels and it was captured on July 6, 2018 at 120 m. Its color composite can be seen in Figure 8g.

The construction of accurate reference data was a long-term process involving forestry experts and the authors of the paper. Information from vegetation inventories, field visits and the expertise of the forestry experts along with the analysis of canopy textures were the main elements considered in producing the reference data. The latest revisions of the reference maps for the River Oitavén, Creek Ermidas, Xesta Basin, and Eiras Dam datasets can be seen in Figures 8b, 8d, 8f, and 8h, respectively. The color legend and pixel count for the different classes are detailed in Table 1.

T

Table 1: Color code and disaggregated pixel count of the reference data by class and dataset.

#	Color	Class	River Oitavén	Creek Ermidas	Eiras Dam	Xesta Basin
0.	■	Unknown	38,879,694	219,303,651	90,270,115	139,955,174
1.	■	Water	309,248	163,930	734,617	71,756
2.	■	Oak	1,374,889	804,040	2,067,380	3,821,501
3.	■	Tiles	78,785	138,678	8,232	—
4.	■	Meadows	2,440,331	3,423,506	773,964	12,468,609
5.	■	Asphalt	43,861	737,409	85,209	130,612
6.	■	Bare Soil	113,329	123,416	96,935	49,468
7.	■	Rock	79,152	174,088	144,800	503,776
8.	■	Concrete	128,022	32,866	27,061	—
9.	■	Autochthonous Vegetation	458,565	—	—	—
10.	■	Eucalyptus	863,698	1,135,997	8,451	—
11.	■	Pines	193,884	184,547	95,132	—

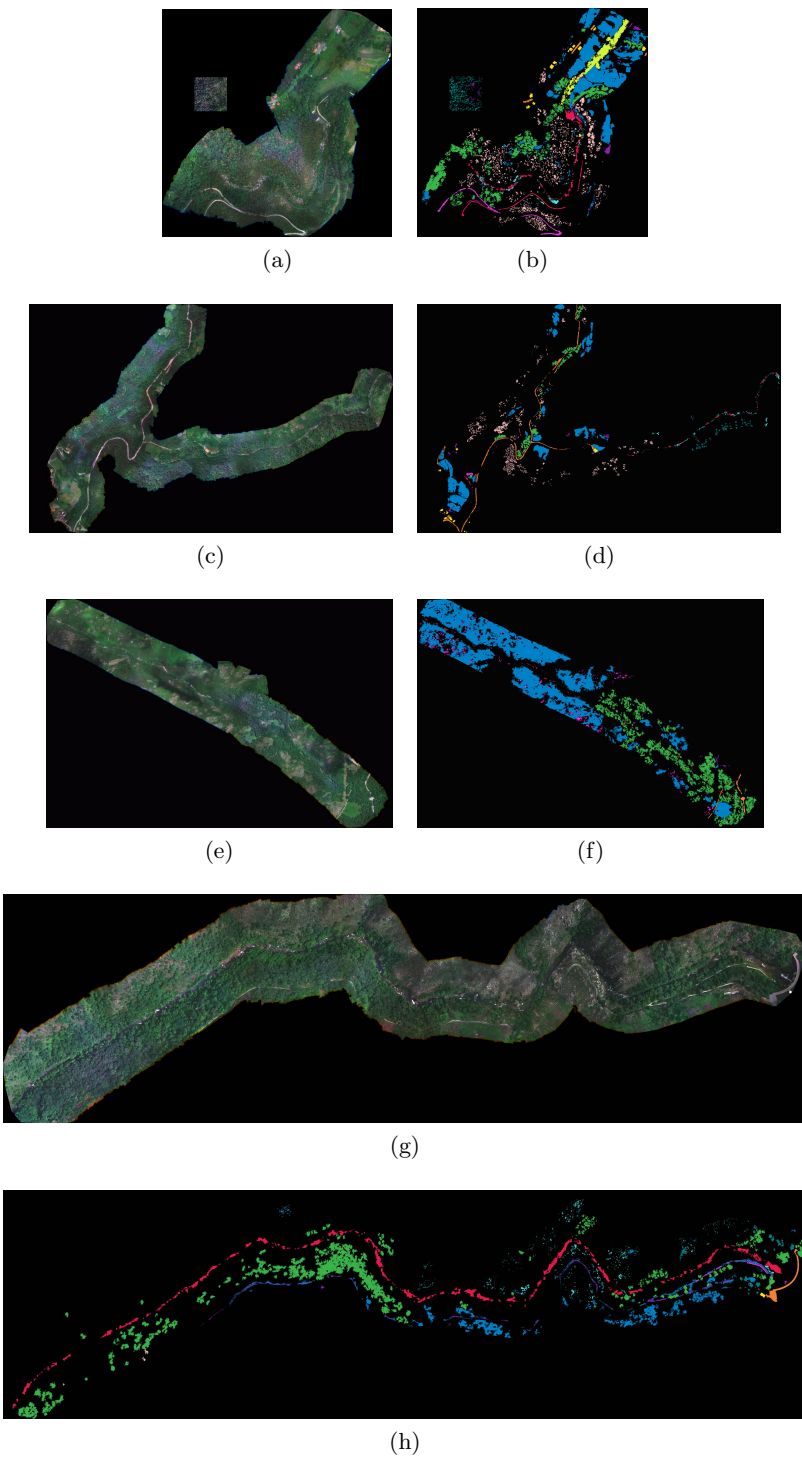


Figure 8: Multispectral datasets obtained for the experimental study. The color composite of figures (a), (c), (e) and (g) alongside the reference data of (b), (d), (f) and (h) correspond to the River Oitavén, Creek Ermidas, Eiras Dam, and Xesta Basin datasets, respectively.

#### 4. EXPERIMENTAL RESULTS

We evaluate the classification scheme in terms of Overall Accuracy (OA) and Average Accuracy (AA). OA represents the total percentage of correctly classified pixels. AA represents the average percentage of correctly classified pixels for each class.

In this section we present the experimental results of the proposed scheme tuned using segments with an average size of 400 pixels, regularisation factor of 20, 200 iterations for the SLIC algorithm. For  $k$ -means the number of centroids that is the same as the number of clusters is 30. Finally, for the EMP, 12 bands are generated by using circular structuring elements of sizes 2, 4, 8, 10, 12 and 14. The values for these parameters were selected after an extensive search considering the four real datasets.

In order to perform a supervised classification by SVM, the pixels in the reference data are usually divided into two sets, training and testing. In our case the number of pixels of the image is reduced by using only one superpixel to characterize each segment obtained by SLIC. Table 2 details the number of randomly selected pixels (Sel. in the table) the total number of pixels, and the corresponding numbers of segments. As a regular rule, we selected for training purposes only 15 % of the total number of segments for large classes such as Oak or Meadows, and between 20 % and 30 % for the smallest ones (Tiles, Concrete).

Class	River Oitavén				Creek Ermidas				Eiras Dam				Xesta Basin			
	Pixels		Segments		Pixels		Segments		Pixels		Segments		Pixels		Segments	
	Sel.	Total	Sel.	Total	Sel.	Total	Sel.	Total	Sel.	Total	Sel.	Total	Sel.	Total	Sel.	Total
Water	52,827	309,248	96	643	26,435	163,930	48	321	113,319	734,617	214	1,428	10,747	71,756	20	146
Oak	209,344	1,374,889	554	3,696	124,614	804,040	331	2,209	317,454	2,067,380	859	5,732	444,515	3,821,501	1,103	9,878
Tiles	12,548	78,785	27	186	19,911	138,678	45	303	3,262	8,232	8	20	—	—	—	—
Meadows	368,637	2,440,331	903	6,025	530,229	3,423,506	1,273	8,489	106,951	773,964	271	1,813	1,370,935	12,468,609	3,377	31,214
Asphalt	6,977	43,861	14	95	114,028	737,409	255	1,704	13,765	85,209	30	181	17,017	130,612	40	324
Bare Soil	16,841	113,329	43	287	19,353	123,416	47	315	19,448	96,935	55	331	9,989	49,468	25	122
Rock	10,829	79,152	32	218	22,732	174,088	67	447	11,018	144,800	40	217	50,617	503,776	151	1,368
Concrete	20,316	128,022	55	369	4,362	32,866	12	80	9,148	27,061	25	84	—	—	—	—
N. Vegetation	70,758	458,565	190	1,273	—	—	—	—	—	—	—	—	—	—	—	—
Eucalyptus	121,074	863,698	402	2,684	168,238	1,135,997	484	3,230	2,691	8,451	8	24	—	—	—	—
Pines	26,386	193,884	68	458	27,742	184,547	77	516	19,346	95,132	55	265	—	—	—	—

Table 2: Training samples and total number of samples of the reference data used in the experiments. The values are shown in terms of pixels and the corresponding reduced number of segments.

A comparison of the SVM accuracy classification results yielded by a pixel-wise SVM classification and by the proposed scheme when segments are classified, is shown in Table 3. As it can be seen, an increase in OA and AA of 15 % and 7 %, respectively, is observed. The aforementioned results are remarkable in the sense that the benefits of using spatial information are verified despite the reduction in the amount of training features. Moreover, on the right part of the table, the OA values obtained by each SVM of the classification hierarchy are detailed. The accuracies for the two classifiers that perform the first separation of segments identifying vegetation and water (SVM 1 and SVM 2 respectively), achieved very high OA values. These high values are very relevant to reduce the number of mistakes produced by the last two specialised classifiers. The variation in the amount of samples available for the different classes and the different datasets produce a variation in the OA values depending on the dataset considered.

Dataset	SVM				Scheme							
	OA	AA	OA	AA	SVM 1	SVM 2	SVM 3	SVM 4				
River Oitavén	72.26 %	77.68 %	88.40 %	86.39 %	98.86 %	99.72 %	89.99 %	88.20 %				
Creek Ermidas	78.78 %	81.65 %	94.43 %	89.73 %	99.76 %	99.70 %	93.97 %	94.53 %				
Eiras Dam	79.93 %	81.18 %	93.84 %	87.30 %	99.39 %	99.70 %	95.05 %	93.49 %				
Xesta Basin	82.04 %	81.05 %	94.61 %	86.21 %	99.46 %	99.89 %	87.96 %	94.92 %				

Table 3: Comparison in terms of classification accuracy of the proposed scheme and a SVM classification.

## 5. CONCLUSIONS

The problem of making an inventory of the vegetation species present at the river banks in order to control natural resources is studied in this paper. In particular, a spatial-spectral texture-based classification scheme for the identification of vegetation species from multispectral images is presented. The scheme was developed to adapt to the identification of vegetation species, mainly trees, and non-vegetation classes such as water, rocks and artificial structures present in the river banks of Galicia, in Spain. The work was carried out to replace inventories based on field visits that are costly in time and money, because experts need to walk over large areas that are difficult to access.

The scheme consists of different steps. The spectral-spatial information is extracted by using a superpixel segmentation algorithm called SLIC, and extended morphological profiles. Texture features are extracted by using a  $k$ -means algorithm and selectively applied only to the classification of vegetation. The supervised classification is performed by a hierarchical structure made up of four SVM classifiers and is featured not over pixels but over superpixels that represent the segments obtained by the SLIC algorithm, thus reducing the computational time.

The proposed scheme requires accurate reference data as input. It was evaluated over 4 multispectral datasets obtained by a UAV at a height of 120 meters, showing its suitability to obtain relevant results for the forestry experts. In particular, accuracies of up to 94.61% were obtained in comparison to values of up to 82.04% in the case of a standard SVM classifier.

As future work we plan to analyse more in detail the performance of the classification scheme when different images obtained by the same sensor in different spatial locations are analyzed.

## ACKNOWLEDGMENTS

This work was supported in part by the Civil Program UAVs Initiative, promoted by the Xunta de Galicia and developed in partnership with the Babcock company to promote the use of unmanned technologies in civil services. We also have to acknowledge the support by the Consellería de Educación, Universidade e Formación Profesional [grant numbers GRC2014/008, ED431C 2018/19, and ED431G/08], Ministerio de Economía y Empresa, Government of Spain [grant number TIN2016-76373-P] and by Junta de Castilla y León - ERDF (PROPHET Project) [grant number VA082P17]. All are co-funded by the European Regional Development Fund (ERDF).

## REFERENCES

- [1] Xue, J. and Su, B., "Significant remote sensing vegetation indices: A review of developments and applications," *Journal of Sensors* **2017** (2017).
- [2] Maggiori, E., Plaza, A., and Tarabalka, Y., *[Models for Hyperspectral Image Analysis: From Unmixing to Object-Based Classification]*, 37–80, Springer International Publishing, Cham (2018).
- [3] Senthilnath, J., Kandukuri, M., Dokania, A., and Ramesh, K., "Application of UAV imaging platform for vegetation analysis based on spectral-spatial methods," *Computers and Electronics in Agriculture* **140**, 8 – 24 (2017).
- [4] Feng, Q., Liu, J., and Gong, J., "Uav remote sensing for urban vegetation mapping using random forest and texture analysis," *Remote sensing* **7**(1), 1074–1094 (2015).
- [5] Fu, Y., Zhao, C., Wang, J., Jia, X., Yang, G., Song, X., and Feng, H., "An improved combination of spectral and spatial features for vegetation classification in hyperspectral images," *Remote Sensing* **9**(3) (2017).
- [6] Szantoi, Z., Escobedo, F., Abd-Elrahman, A., Smith, S., and Pearlstine, L., "Analyzing fine-scale wetland composition using high resolution imagery and texture features," *International Journal of Applied Earth Observation and Geoinformation* **23**, 204–212 (2013).
- [7] Benediktsson, J. A., Palmason, J. A., and Sveinsson, J. R., "Classification of hyperspectral data from urban areas based on extended morphological profiles," *IEEE Transactions on Geoscience and Remote Sensing* **43**, 480–491 (March 2005).
- [8] Argüello, F. and Heras, D. B., "ELM-based spectral-spatial classification of hyperspectral images using extended morphological profiles and composite feature mappings," *International Journal of Remote Sensing* **36**(2), 645–664 (2015).

- [9] Achanta, R., Shaji, A., Smith, K., Lucchi, A., Fua, P., and Süstrunk, S., "SLIC superpixels compared to state-of-the-art superpixel methods," *IEEE Transactions on Pattern Analysis and Machine Intelligence* **34**, 2274–2282 (Nov 2012).
- [10] Clausi, D. A., "K-means iterative fisher unsupervised clustering algorithm applied to image texture segmentation," *Pattern Recognition* **35**(9), 1959–1972 (2002).
- [11] Macqueen, J., "Some methods for classification and analysis of multivariate observations," in [*In 5-th Berkeley Symposium on Mathematical Statistics and Probability*], 281–297 (1967).
- [12] Jégou, H., Douze, M., Schmid, C., and Pérez, P., "Aggregating local descriptors into a compact image representation," in [*2010 IEEE Computer Society Conference on Computer Vision and Pattern Recognition*], 3304–3311 (June 2010).
- [13] Sánchez, J., Perronnin, F., Mensink, T., and Verbeek, J., "Image classification with the Fisher vector: Theory and practice," *International Journal of Computer Vision* **105**, 222–245 (Dec 2013).